Mathematical Biosciences and Engineering

https://www.aimspress.com/journal/mbe

MBE, 21(4): 5032–5046.
DOI: 10.3934/mbe.2024222
Received: 18 December 2023
Revised: 13 February 2024
Accepted: 18 February 2024
Published: 04 March 2024

Research article

Predefined-time sliding mode control of chaotic systems based on disturbance observer

Yun Liu[1] **and Yuhong Huo**[2,*]

[1] School of Electronic Engineering, Huainan Normal University, Huainan 232038, China
[2] School of Finance and Mathematics, Huainan Normal University, Huainan 232038, China

* **Correspondence:** Email: yuhonghuo@hnnu.edu.cn.

Abstract: In this paper, in order to realize the predefined-time control of n-dimensional chaotic systems with disturbance and uncertainty, a disturbance observer and sliding mode control method were presented. A sliding manifold was designed for ensuring that when the error system runs on it, the tracking error was stable within a predefined time. A sliding mode controller was developed which enabled the dynamical system to reach the sliding surface within a predefined time. The total expected convergence time can be acquired through presetting two predefined-time parameters. The results demonstrated the feasibility of the proposed control method.

Keywords: predefined-time control; sliding mode control; chaotic system; disturbance observer

1. Introduction

Chaos refers to the irregular motion that occurs in a deterministic system, which is characterized by extremely sensitive initial conditions, inherent randomness, complexity and unpredictability. In chaotic systems (CSs), when the initial states of identical oscillators change slightly, their future states are usually different [1]. Pecora and Carol achieved outstanding research results in 1990 [2], and since then chaos synchronization has become a research hotspot, drawing wide heed from scientists, and being widely used in many fields of secure communication, network synchronization and control engineering [3–5]. In [6], a sliding mode control (SMC) method was proposed to synchronize unified CSs. In [7], an improved global nonlinear integral SMC method was developed to synchronize CSs with external disturbances and internal uncertainties. In [8], an extended state observer was developed to synchronize CSs based on linear differential equations. It should be emphasized that the above synchronization error is asymptotically stable, that is, the synchronization time may be relatively long.

Many industrial processes have higher requirements for convergence time, so finite-time stability has been proposed by many scholars. Different from the asymptotic-time control, finite-time control

ensures that the synchronization error converges to origin within a finite time, and has the characteristics of higher convergence accuracy and faster convergence rate, which is an important breakthrough. In [9], under finite-time control theory, Cai et al. were committed to actualizing generalized synchronization of fractional order CSs. In [10], an SMC method was proposed to design a controller to ensure that uncertain complex CSs can synchronize in a finite time under network transmission. In [11], Ao et al. utilized an impulsive control method to synchronize CSs in a predefined time. In [12], a synchronization controller was designed to ensure that two CSs with different dimensions can synchronize in a finite time. However, the finite-time control suffers from some issues, for instance, the settling time is subject to the initial conditions. The initial value is often unknown in practice and cannot be set arbitrarily, which greatly increases difficulty of minimizing the synchronization time. When it is arbitrarily large, the synchronization settling time may be arbitrarily large. Therefore, this restricts the practical usage of finite-time control, and to a certain extent, makes finite-time control lack practical significance in industrial production. To address this problem, the fixed-time control [13] is presented. It is characterized by a constant upper bound for settling time, which isn't affected by the initial conditions. For practical systems with convergence time accuracy requirements, this feature advances the practical usage of fixed-time control. In [14], a terminal SMC method was applied to actualize the fixed-time synchronization between two identical CSs. In [15], a control strategy which isn't the same as the present adaptive design methods was developed for researching the fixed-time tracking control in nonlinear systems. However, there are also two main problems with fixed-time control. For one thing, it needs to calculate the boundary of the settling time. For another thing, it is conservative for estimating the settling time.

To address the above issues, the predefined-time control is proposed, whose main advantage is that the convergence time is uninflunced by the initial conditions [16, 17]. It not only saves a process, which is to calculate the boundary of settling time, but also adjusts the predefined-time parameters by changing the system parameters. In recent years, scholars have also made a lot of efforts on predefined-time synchronization (PTS) of CSs. In [18], a simplified control inputs method was developed to achieve PTS of memristor CSs. In [19], under predefined-time stability theory, a control method was presented to realize the PTS of CSs. In [20], by designing a synchronization controller, PTS of a chaotic system at different dimensions was successfully achieved. It should be noted that the model of the aforementioned chaotic system should be known in advance.

It is well known that SMC is an effective nonlinear control method for uncertain systems due to its anti-interference ability and robustness. There are also some related works [21–27] on PTS of CSs using SMC. In [21], under the PTS theory, a novel fast terminal SMC scheme was developed to synchronize two different multi-input and multi-output CSs. An active controller was developed to ensure that two CSs achieved PTS, where a new sliding surface was designed in [22]. In [23], aming to achieve fast and accurate synchronization of CSs within a predefined time, an SMC method was proposed. In [24], Zhang et al. presented an SMC method to achieve PTS of CSs, where a sliding mode synchronization controller was developed to guarantee that the dynamic system is capable of reaching the sliding surface within a predefined time; however, its sliding surface is relatively complex, and the shaking phenomenon is obvious. Therefore, further research is needed on how to design a simple and practical sliding surface to track and control CSs within a predefined time.

Based on the above discussion, there are three points that need to be further explored regarding the control of CSs : 1) These references have a hypothesis that the upper bounds of external disturbances

and internal uncertainties are known, but may be unknown in practice. How to design a predefined-time control for CSs under these unknown conditions has become a research focus. 2) If the internal uncertainty and external disturbances of the system are regarded as a mixed disturbance, the design of disturbance observer becomes necessary. 3) Due to the use of the sliding mode control method, further research is needed on how to reduce the chattering phenomenon of the sliding mode controller.

Recently, significant research results have been obtained on optimal control of nonlinear systems [28–31], For example, in [28], an output feedback algebraic Riccati equation was constructed to design an output feedback optimal control strategy for nonlinear systems. A hybrid hierarchical classification algorithm was proposed in [30]. Therefore, based on the above work on the design of observer and adaptive law, the main contributions of this article are as follows: (*I*) Develop a disturbance observer that can effectively estimate the mixed disturbance. (*II*) A new sliding surface is presented, and it enables the tracking error to reach a small neighborhood of zero at the origin within a predefined time when the tracking error runs on it. (*III*) The chattering phenomenon of the controller is greatly reduced. The remaining of this article is arranged following. Section 2 introduces preliminaries and problem descriptions. The development of sliding surface and controller are included in Section 3. Examples in Section 4 are provided to verify the efficiency of the presented method. Conclusions are provided in Section 5.

2. Preliminaries and system description

Consider the following n-dimensional CSs

$$\begin{cases} \dot{\zeta}_1 = g_1(\boldsymbol{\zeta}) + \Delta g_1(\boldsymbol{\zeta}) + d_1 + u_1, \\ \dot{\zeta}_2 = g_2(\boldsymbol{\zeta}) + \Delta g_2(\boldsymbol{\zeta}) + d_2 + u_2, \\ \vdots \\ \dot{\zeta}_n = g_n(\boldsymbol{\zeta}) + \Delta g_n(\boldsymbol{\zeta}) + d_n + u_n, \end{cases} \tag{2.1}$$

where $\boldsymbol{\zeta} = [\zeta_1, \zeta_2, \cdots, \zeta_n]^T \in \mathbb{R}^n$ is measurable system state. $g_i(\boldsymbol{\zeta}) : \mathbb{R}^n \to \mathbb{R}$ is the continuous nonlinear function, $\Delta g_i(\boldsymbol{\zeta}) : \mathbb{R}^n \to \mathbb{R}$ is the internal uncertainty and $d_i : \mathbb{R} \to \mathbb{R}$ is the external disturbance. $u = [u_1, u_2, \cdots, u_n]^T \in \mathbb{R}^n$ is the control input vector.

Assumption 1. *Assume that the continuous nonlinear function $g_i(\boldsymbol{\zeta})$, the internal uncertainty $\Delta g_i(\boldsymbol{\zeta})$ and the external disturbance d_i are unknown and bounded, $i = 1, 2, \cdots, n$.*

Remark 1. *In [22–27], the internal uncertainty $\Delta g_i(\boldsymbol{\zeta})$ satisfies $|\Delta g_i(\boldsymbol{\zeta})| \leq \varphi_i \|\boldsymbol{\zeta}\|$, and the external disturbance d_i satisfies $|d_i| \leq C_i$. The nonlinear continuous function $g_i(\boldsymbol{\zeta})$ and positive constants φ_i and C_i are known. In contrast, this paper only assumes that $g_i(\boldsymbol{\zeta})$, $\Delta g_i(\boldsymbol{\zeta})$ and d_i are bounded. Based on this condition, we will design the disturbance observer $\hat{d}_i(t, \boldsymbol{\zeta})$ to estimate $g_i(\boldsymbol{\zeta}) + \Delta g_i(\boldsymbol{\zeta}) + d_i$.*

Define $\boldsymbol{x}_d = [x_{d_1}, x_{d_2}, \cdots, x_{d_n}]^T$ as the reference signal and the tracking error is defined as $\boldsymbol{z} = [z_1, z_2, \cdots, z_n]^T = [\zeta_1 - x_{1d}, \zeta_2 - x_{2d}, \cdots, \zeta_n - x_{nd}]^T$. The system (2.1) and the tracking error system can

be written as

$$\begin{cases} \dot{\zeta}_1 &= \bar{d}_1(t,\boldsymbol{\zeta}) + u_1, \\ \dot{\zeta}_2 &= \bar{d}_2(t,\boldsymbol{\zeta}) + u_2, \\ \vdots & \\ \dot{\zeta}_n &= \bar{d}_n(t,\boldsymbol{\zeta}) + u_n, \end{cases} \tag{2.2}$$

and

$$\begin{cases} \dot{z}_1 &= \bar{d}_1(t,\boldsymbol{\zeta}) - \dot{x}_{d_1} + u_1, \\ \dot{z}_2 &= \bar{d}_2(t,\boldsymbol{\zeta}) - \dot{x}_{d_2} + u_2, \\ \vdots & \\ \dot{z}_n &= \bar{d}_n(t,\boldsymbol{\zeta}) - \dot{x}_{d_n} + u_n, \end{cases} \tag{2.3}$$

where $\bar{d}_i(t,\boldsymbol{\zeta}) = g_i(\boldsymbol{\zeta}) + \Delta g_i(\boldsymbol{\zeta}) + d_i$.

Definition 1 (Finite time stability [32])**.** *Assume that the sysnchronization error system* (2.3) *is asymptotically stable and any solution $\boldsymbol{z}(t,\boldsymbol{z}_0)$ reaches the equilibrium point in a finite time, i.e.,*

$$\lim_{t\to T(\boldsymbol{z}_0)} \|\boldsymbol{z}\| = \lim_{t\to T(\boldsymbol{z}_0)} \|\boldsymbol{\zeta} - \boldsymbol{x}_d\| = 0, \tag{2.4}$$

then the error system (2.3) *is a finite-time stability. $T(\boldsymbol{z}_0)$ is the settling time, which depends on the initial value z_0.*

Definition 2 (Fixed time stability [33])**.** *Assume that the error system* (2.3) *is globally finite-time stable. If the settling time $T(\boldsymbol{z}_0)$ is bounded, namely, there is a constant $T_{max}> 0$ such that $T(\boldsymbol{z}_0) \le T_{max}$ for all $\boldsymbol{z}_0 \in \mathbb{R}^n$, then the error system* (2.3) *is a fixed-time stability.*

Definition 3 (Predefined-time stability [34])**.** *Assume that the error system* (2.3) *is globally fixed-time stable. If the settling time $T(\boldsymbol{z}_0)$ satisfies $T(\boldsymbol{z}_0) \le T_c$ for all $\boldsymbol{z}_0$, where $T_c > 0$ is a predefined time, then the error system* (2.3) *is a predefined-time stability.*

Remark 2. *In contrast to finite-time stability, predefined-time stability is unaffected by initial conditions. It is superior than fixed-time stability because it can pre-allocate the boundary of the settling time, saving time in calculating the boundary of the settling time, making theoretical analysis simpler and estimating convergence time more accurately.*

For the sake of better deterring whether a dynamic system is a predefined-time stability, the following conclusion needs to be used in this article.

Lemma 1 ([35])**.** *If the system $\dot{\varsigma} = \phi(t,\varsigma)$ is a finite-time stability and a Lyapunov function $V(t)$ satisfies*

$$\dot{V} \le -\frac{\pi}{2qT_c}(V^{1-q} + V^{1+q}), \tag{2.5}$$

then $\dot{\varsigma} = \phi(t,\varsigma)$ is a predefined-time stability, where $T_c> 0$ is a predefined time and $q \in (0, \frac{1}{2})$.

Proof. The settling time implies that $V(t)$ with an initial value $V_0 > 0$ converges to $V_f = 0$ in the time $T(\varsigma_0)$. From (2.5), one obtains

$$T(\varsigma_0) \le -\frac{2qT_c}{\pi}\int_{V_0}^{V_f} \frac{dV}{V^{1-q} + V^{1+q}}$$

$$
\begin{aligned}
=&\frac{2qT_c}{\pi}\int_{V_f}^{V_0}\frac{dV}{V^{1-q}+V^{1+q}}\\
=&\frac{2T_c}{\pi}\int_{V_f}^{V_0}\frac{dV^q}{1+(V^q)^2}\\
\leq&T_c[\frac{2}{\pi}\arctan(V_0^q)]\\
\leq&T_c.
\end{aligned}
$$

Notice that $\dot{\varsigma}=\phi(t,\varsigma)$ is finite-time stability and the settling time $T(\varsigma_0)\leq T_c$. Therefore, $\dot{\varsigma}=\phi(t,\varsigma)$ is a predefined-time stability. This completes the proof. ■

Lemma 2 ([36]). *If a Lyapunov function $V(t)$ satisfies*

$$\dot{V}\leq -\frac{\pi}{qT_c}(V^{1-\frac{q}{2}}+V^{1+\frac{q}{2}})+r, \tag{2.6}$$

where $r>0$, then for a given positive constant $\upsilon\triangleq\frac{qrT_c}{\pi}$ that satisfies $V\leq\upsilon$ for all $t>2T_c$, where $T_c>0$ is a predefined time and $q\in(0,1)$.

Lemma 3 ([36]). *If function $f(\boldsymbol{\zeta})$ is continuous on a compact Ω, then $f(\boldsymbol{\zeta})$ can be expressed as*

$$f(\boldsymbol{\zeta})=\theta^{*T}\psi_f(\boldsymbol{\zeta})+\varepsilon(\boldsymbol{\zeta}), \tag{2.7}$$

where θ^* is the ideal parameter vector, $\psi_f(\boldsymbol{\zeta})$ is the fuzzy basis function vector, $\varepsilon(\boldsymbol{\zeta})$ is the fuzzy estimation error such that $|\varepsilon(\boldsymbol{\zeta})|\leq\varepsilon_f^*$, where ε_f^* is an unknown positive constant.

3. Design of predefined-time control scheme

3.1. Design of the disturbance observer

In order to estimate the unknown function $\bar{d}_i(t,\boldsymbol{\zeta})$, the following observer is designed:

$$
\begin{cases}
\hat{d}_i(t,\boldsymbol{\zeta})=-\beta_i s_i+\hat{\theta}_{f_i}^T\psi_{f_i}(\boldsymbol{\zeta}),\\
s_i=w_i-\zeta_i,\\
\dot{w}_i=-\beta_i s_i+\hat{\theta}_{f_i}^T\psi_{f_i}(\boldsymbol{\zeta})+u_i,
\end{cases} \tag{3.1}
$$

where β_i is a design positive parameter and $\hat{\theta}_{f_i}^T\psi_{f_i}(\boldsymbol{\zeta})$ is an estimate of $\theta_{f_i}^{*T}\psi_{f_i}(\boldsymbol{\zeta})$ ($\theta_{f_i}^{*T}\psi_{f_i}(\boldsymbol{\zeta})=\bar{d}_i(t,\boldsymbol{\zeta})-\varepsilon_{f_i}(\boldsymbol{\zeta})$ by using Lemma 3). Define the estimation error $\tilde{d}_i(t,\boldsymbol{\zeta})=\hat{d}_i(t,\boldsymbol{\zeta})-\tilde{d}_i(t,\boldsymbol{\zeta})$. One has

$$
\begin{aligned}
\tilde{d}_i(t,\boldsymbol{\zeta})&=\hat{d}_i(t,\boldsymbol{\zeta})-\tilde{d}_i(t,\boldsymbol{\zeta})\\
&=-\beta_i s_i+\hat{\theta}_{f_i}^T\psi_{f_i}(\boldsymbol{\zeta})+u_i-\dot{\zeta}_i\\
&=\dot{w}_i-\dot{z}_i=\dot{s}_i.
\end{aligned} \tag{3.2}
$$

Theorem 1. *For the system* (2.2)*, the observer error $\tilde{d}_i(t,\boldsymbol{\zeta})$ is bounded by using the disturbance observer $\hat{d}_i(t,\boldsymbol{\zeta})$ in* (3.1) *and the adaptive law as*

$$\dot{\hat{\theta}}_{f_i}=\rho_i(-s_i\psi_{f_i}(\boldsymbol{\zeta})-\lambda_i\hat{\theta}_{f_i}), \tag{3.3}$$

where ρ_i,λ_i are positive constants.

Proof. Consider Lyapunov function $V_{s_i} = \frac{1}{2}s_i^2 + \frac{1}{\rho_i}\tilde{\theta}_{f_i}^T\tilde{\theta}_{f_i}$, where $\tilde{\theta}_{f_i} = \theta_{f_i}^* - \hat{\theta}_{f_i}$. Form (3.1) and (3.3), one has

$$\begin{aligned}\dot{V}_{s_i} &= s_i(\dot{w}_i - \dot{z}_i) - \tfrac{1}{\rho_i}\tilde{\theta}_{f_i}^T\dot{\hat{\theta}}_{f_i}\\ &= -\beta_i s_i^2 + s_i u_i + s_i\hat{\theta}_{f_i}^T\psi_{f_i}(\boldsymbol{\zeta}) - s_i\theta_{f_i}^{*T}\psi_{f_i}(\boldsymbol{\zeta})\\ &\quad -s_i\varepsilon_{f_i}(\boldsymbol{\zeta}) - s_i u_i - \tilde{\theta}_{f_i}^T(-s_i\psi_{f_i}(\boldsymbol{\zeta}) - \lambda_i\hat{\theta}_{f_i})\\ &= -\beta_i s_i^2 - s_i\varepsilon_{f_i}(\boldsymbol{\zeta}) + \lambda_i\tilde{\theta}_{f_i}^T\hat{\theta}_{f_i}\\ &\le -(\beta_i - \tfrac{1}{4})s_i^2 + \varepsilon_{f_i}^* - \tfrac{\lambda_i}{2}\tilde{\theta}_{f_i}^T\tilde{\theta}_{f_i} + \tfrac{\lambda_i}{2}\|\theta_{f_i}^*\|^2.\end{aligned} \tag{3.4}$$

Let $r_{i1} = \varepsilon_{f_i}^* + \frac{\lambda_i}{2}\|\theta_{f_i}^*\|^2$. Select β_i such as $\beta_i > \frac{1}{4}$ and define the following compact sets: $\Omega_{s_i} = \{s_i| \, |s_i| \le \sqrt{\frac{r_{1i}}{\beta_i - \frac{1}{4}}}\}$ and $\Omega_{\tilde{\theta}_{f_i}} = \{\|\tilde{\theta}_{f_i}\| | \, \|\tilde{\theta}_{f_i}\| \le \sqrt{\frac{2r_{1i}}{\lambda_i}}\}$. Obviously, if $s_i \notin \Omega_{s_i}$ or $\tilde{\theta}_{f_i} \notin \Omega_{\tilde{\theta}_{f_i}}$, one has $\dot{V}(t) < 0$. Thus, s_i and $\tilde{\theta}_{f_i}$ are bounded. When s_i and $\tilde{\theta}_{f_i}$ are limited within the small compact sets Ω_{s_i} and $\Omega_{\tilde{\theta}_{f_i}}$, respectively, then $\dot{s}_i = -\beta_i s_i - \tilde{\theta}_{f_i}^T\psi_{f_i}(\boldsymbol{\zeta}) - \varepsilon_{f_i}(\boldsymbol{\zeta})$ is also bounded, that is, there exists a positive constant η_i such that $|\dot{s}_i| = |\tilde{d}(t, \boldsymbol{\zeta})| \le \eta_i$. This completes the proof. ■

3.2. Design of the sliding surface and controller

The design idea of this article is divided into two steps: The first step is to design a sliding manifold so that the tracking error can reach the neighborhood of zero on the sliding surface within a predefined time. The second step is to design a controller so that the error system can reach the sliding surface within a predefined time.

In this article, the sliding manifold and the corresponding controller are designed as follows:

$$\begin{aligned}\sigma_i &= z_i + s_i + \int_0^t (\tfrac{1}{q_1}\tfrac{\pi}{T_{c_1}}(\tfrac{1}{2})^{1-\frac{q_1}{2}}\mathrm{sgn}(z_i(\tau))|z_i(\tau)|^{1-q_1}\\ &\quad + \tfrac{1}{q_1}\tfrac{\pi}{T_{c_1}}(\tfrac{1}{2})^{1+\frac{q_1}{2}}\mathrm{sgn}(z_i(\tau))|z_i(\tau)|^{1+q_1} + \tfrac{z_i(\tau)}{2})\mathrm{d}\tau,\end{aligned} \tag{3.5}$$

and

$$\begin{aligned}u_i &= \dot{x}_{d_i} - \hat{d}_i(t, \boldsymbol{\zeta}) - \tfrac{1}{q_1}\tfrac{\pi}{T_{c_1}}(\tfrac{1}{2})^{1-\frac{q_1}{2}}\mathrm{sgn}(z_i)|z_i|^{1-q_1} - \tfrac{1}{q_1}\tfrac{\pi}{T_{c_1}}(\tfrac{1}{2})^{1+\frac{q_1}{2}}\mathrm{sgn}(z_i)|z_i|^{1+q_1}\\ &\quad -\tfrac{z_i(\tau)}{2} - \tfrac{1}{q_2}\tfrac{\pi}{T_{c_2}}(\tfrac{1}{2})^{2-q_2}\mathrm{sgn}(\sigma_i)|\sigma_i|^{1-2q_2}\\ &\quad -\tfrac{1}{q_2}\tfrac{\pi}{T_{c_2}}(\tfrac{1}{2})^{2+q_2}\mathrm{sgn}(\sigma_i)|\sigma_i|^{1+2q_2},\end{aligned} \tag{3.6}$$

where T_{c_1}, T_{c_2} are predefined times and $q_1 \in (0, 1)$, $q_2 \in (0, \frac{1}{2})$.

The following theorem states the primary result.

Theorem 2. *If the controller is chosen as* (3.6)*, then the synchronization system* (2.3) *will reach the sliding surface* $\sigma_i = 0$ *within the predefined time* T_{c_2}.

Proof. Select a Lyapunov function as $V_{\sigma_i} = \frac{1}{2}\sigma_i^2$, then

$$\begin{aligned}\dot{V}_{\sigma_i} &= \sigma_i \cdot \dot{\sigma}_i\\ &= \sigma_i(\bar{d}_i(t, \boldsymbol{\zeta}) - \dot{x}_{d_i} + u_i - \dot{s}_i + \tfrac{1}{q_1}\tfrac{\pi}{T_{c_1}}(\tfrac{1}{2})^{1-\frac{q_1}{2}}\mathrm{sgn}(z_i)|z_i|^{1-q_1}\\ &\quad + \tfrac{1}{q_1}\tfrac{\pi}{T_{c_1}}(\tfrac{1}{2})^{1+\frac{q_1}{2}}\mathrm{sgn}(z_i)|z_i|^{1+q_1})\\ &= \sigma_i(-\tilde{d}_i(t, \boldsymbol{\zeta}) - \dot{s}_i - \tfrac{1}{q_2}\tfrac{\pi}{T_{c_2}}(\tfrac{1}{2})^{2-q_2}\mathrm{sgn}(\sigma_i)|\sigma_i|^{1-2q_2}\\ &\quad -\tfrac{1}{q_2}\tfrac{\pi}{T_{c_2}}(\tfrac{1}{2})^{2+q_2}\mathrm{sgn}(\sigma_i)|\sigma_i|^{1+2q_2}).\end{aligned} \tag{3.7}$$

Notice that $\dot{s}_i = \tilde{d}_i(t, \boldsymbol{\zeta})$. One gets

$$\dot{V}_{\sigma_i} = -\frac{\pi}{2q_2 T_{c_2}}(V_{\sigma_i}^{1-q_2} + V_{\sigma_i}^{1+q_2}) < 0. \tag{3.8}$$

By using Lemma 1, the tracking system (2.3) will reach the sliding surface $\sigma_i = 0$ within the predefined time T_{c_2}. This completes the proof. ■

When the tracking error system (2.3) is limited on the sliding surface $\sigma_i = 0$, one has $\dot{\sigma}_i = 0$, that is

$$\begin{aligned} \dot{\sigma}_i \ &= \dot{z}_i + \dot{s}_i + \frac{1}{q_1}\frac{\pi}{T_{c_1}}(\tfrac{1}{2})^{1-\frac{q_1}{2}}\mathrm{sgn}z_i(\tau)|z_i(\tau)|^{1-q_1} \\ &\quad + \frac{1}{q_1}\frac{\pi}{T_{c_1}}(\tfrac{1}{2})^{1+\frac{q_1}{2}}\mathrm{sgn}z_i(\tau)|z_i(\tau)|^{1+q_1} + \tfrac{z_i}{2} = 0,\ t \geq T_{c_2}. \end{aligned} \tag{3.9}$$

From (3.9), the sliding surface $\sigma_i = 0$ can guarantee that when the error system (2.3) runs on it, the tracking error z_i is stable within $2T_{c_1}$. The following theorem is given as below.

Theorem 3. *If the tracking error system* (2.3) *runs on the sliding surface $\sigma_i = 0$, then the tracking error z_i will converge to the neighborhood of zero within the predefined time $2T_{c_1}$.*

Proof. According to (3.9), if the tracking error system (2.3) moves on the sliding surface $\sigma_i = 0$ after T_{c_2}, one has $\dot{\sigma}_i = 0$, so

$$\dot{z}_i = -\frac{1}{q_1}\frac{\pi}{T_{c_1}}(\frac{1}{2})^{1-\frac{q_1}{2}}\mathrm{sgn}(z_i)|z_i|^{1-q_1} - \frac{1}{q_1}\frac{\pi}{T_{c_1}}(\frac{1}{2})^{1+\frac{q_1}{2}}\mathrm{sgn}(z_i)|z_i|^{1+q_1} - \frac{z_i^2}{2} - \dot{s}_i.$$

Let $V_{z_i} = \frac{1}{2}z_i^2$, then one has

$$\begin{aligned} \dot{V}_{z_i} =& z_i \cdot \dot{z}_i \\ =& -z_i(\frac{1}{q_1}\frac{\pi}{T_{c_1}}(\frac{1}{2})^{1-\frac{q_1}{2}}\mathrm{sgn}(z_i)|z_i|^{1-q_1} + \frac{1}{q_1}\frac{\pi}{T_{c_1}}(\frac{1}{2})^{1+\frac{q_1}{2}}\mathrm{sgn}(z_i)|z_i|^{1+q_1} + \frac{z_i}{2} + \dot{s}_i) \\ \leq& -\frac{1}{T_{c_1}}\frac{\pi}{q_1}(V_{z_i}^{1-\frac{q_1}{2}} + V_{z_i}^{1+\frac{q_1}{2}}) - \frac{z_i^2}{2} + \frac{z_i^2}{2} + \frac{\eta_i^2}{2} \\ =& -\frac{1}{T_{c_1}}\frac{\pi}{q_1}(V_{z_i}^{1-\frac{q_1}{2}} + V_{z_i}^{1+\frac{q_1}{2}}) + \frac{\eta_i^2}{2}. \end{aligned}$$

By using Lemma 2, one has $V_{z_i} = \frac{1}{2}z_i^2 \leq \frac{q_1 T_{c_1}\eta_i^2}{2\pi}$ within $2T_{c_1}$, that is, $|z_i| \leq \sqrt{\frac{q_1 T_{c_1}\eta_i^2}{\pi}}$, $t \geq 2T_{c_1} + T_{c_2}$. Thus, the proof of Theorem 3 is complete. ■

Remark 3. *According to the results of Theorem 1–3, it can be concluded that the tracking error z_i will approach $\Omega_{z_i} = \{z_i \,|\, |z_i| \leq \sqrt{\frac{q_1 T_{c_1}\eta_i^2}{\pi}}\}$ after the predefined time $2T_{c_1} + T_{c_2}$.*

Remark 4. *In [24], a sliding surface was designed as $s_i = e_i + \int_0^t (c_1 e_i + c_2\mathrm{sgn}(e_i)|e_i|^{1-\alpha} + c_3\mathrm{sgn}(e_i)|e_i|^{1+\alpha} + c_4\mathrm{sgn}(e_i))d\tau$, in which $c_1 = \frac{1}{T_{c_1}}\frac{2}{\alpha}$, $c_2 = \frac{1}{T_{c_1}}\frac{2}{\alpha}(\frac{1}{2})^{1-\frac{\alpha}{2}}$, $c_3 = \frac{1}{T_{c_1}}\frac{2}{\alpha}(\frac{1}{2})^{1+\frac{\alpha}{2}}$, $c_4 > 0$, $\alpha \in (0, 1)$. Compared with the sliding manifold designed in [24], the proposed sliding manifold* (3.5) *consists of an integral term and auxiliary variables, which can ensure robustness and avoid the drawbacks of the common sliding mode approach stage by finding an appropriate initial position to make the system only have a sliding stage.*

4. Numerical simulation

To demonstrate the effectiveness of the proposed method, The Lü system [37] is used as a simulation example to illustrate. The Lü system is described as

$$\begin{cases} \dot{\zeta}_1 = \underbrace{36(\zeta_2 - \zeta_1)}_{g_1(\boldsymbol{\zeta})} + \triangle g_1(\boldsymbol{\zeta}) + d_1 + u_1, \\ \dot{\zeta}_2 = \underbrace{20\zeta_2 - \zeta_1\zeta_3(1 - 2\sin 2\zeta_3)}_{g_2(\boldsymbol{\zeta})} + \triangle g_2(\boldsymbol{\zeta}) + d_2 + u_2, \\ \dot{\zeta}_3 = \underbrace{-3\zeta_3 + \zeta_1\zeta_2}_{g_3(\boldsymbol{\zeta})} + \triangle g_3(\boldsymbol{\zeta}) + d_3 + u_3, \end{cases} \tag{4.1}$$

where the initial values of the system (4.1) are $[\zeta_1(0), \zeta_2(0), \zeta_3(0)]^T = [3, 3, 4]^T$. When $\triangle g_i(\boldsymbol{\zeta}) = 0$, $d_i = 0$ and $u_i = 0$, the phase diagrams of the Lü system are illustrated in Figure 1. The internal uncertainties are $\triangle g_1(\boldsymbol{\zeta}) = 2\zeta_1 \cos t$, $\triangle g_2(\boldsymbol{\zeta}) = 3.5\zeta_2 \cos t$, and $\triangle g_3(\boldsymbol{\zeta}) = 4\zeta_3 \cos t$. d_1, d_2, d_3 are uniformly randomly distributed noise with amplitudes of 3.5.

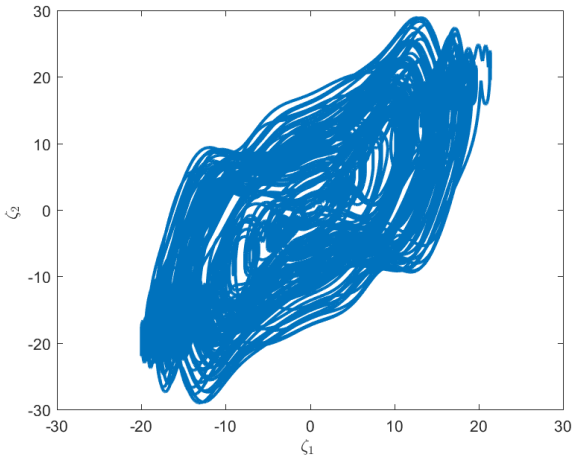

Figure 1. Dynamics of Lü chaotic system.

In this section, we compare our proposed method with the method in [27]. The reference signal is $x_d = [\cos(t), 4\cos(t), 3\cos(t)]^T$.

It should be emphasized that the method in [27] assumes that $g_i(\boldsymbol{\zeta})$ is known and that $\Delta g_i(\boldsymbol{\zeta})$ and d_i satisfy the following inequalities: $|\Delta g_i(\boldsymbol{\zeta})| \leq \varphi_i \|\boldsymbol{\zeta}\|$ and $|d_i| \leq C_i$, where φ_i and C_i are known positive constants, $i = 1, 2, 3$.

Method 1: The predefined-time SMC method in [27] employs (4.2) as the sliding manifold and (4.3) as the controller.

$$\sigma_i = z_i + \int_0^t (b_1 \mathrm{sgn}(z_i(\tau))\,|z_i(\tau)|^{1-\lambda} + b_2 \mathrm{sgn}(z_i(\tau))\,|z_i(\tau)|^{1+\lambda} + b_5 z_i(\tau))d\tau, \tag{4.2}$$

$$\begin{aligned} u_i =& \dot{x}_{d_i} - g_i(\boldsymbol{\zeta}) - b_1 \mathrm{sgn}(e_i)\,|z_i|^{1-\lambda} - b_2 \mathrm{sgn}(z_i)\,|e_i|^{1+\lambda} - b_5 e_i - b_3 \mathrm{sgn}(\sigma_i)\,|\sigma_i|^{1-\lambda} \\ & - b_4 \mathrm{sgn}(\sigma_i)\,|\sigma_i|^{1+\lambda} - b_6\sigma_i - (\phi_i|\zeta_i| + C_i)\mathrm{sgn}(\sigma_i). \end{aligned} \tag{4.3}$$

All parameters in *Method 1* are selected as $\lambda = 0.5$, $T_{c_1} = T_{c_2} = 0.1$, $q_1 = 0.5, q_2 = 0.25$, $b_1 = \frac{1}{q_1}\frac{\pi}{T_{c_1}}(\frac{1}{2})^{1-\frac{q_1}{2}}$, $b_3 = \frac{1}{q_2}\frac{\pi}{T_{c_2}}(\frac{1}{2})^{2-q_2}$, $b_2 = \frac{1}{q_1}\frac{\pi}{T_{c_1}}(\frac{1}{2})^{1+q_1}$, $b_4 = \frac{1}{q_2}\frac{\pi}{T_{c_2}}(\frac{1}{2})^{2+q_2}$, $\phi_1 = 2$, $\phi_2 = 3.5$, $\phi_3 = 4$, $C_1 = C_2 = C_3 = 3.5$, $b_5 = b_6 = 5$. Simulation results of *Method 1* are depicted in Figure 2.

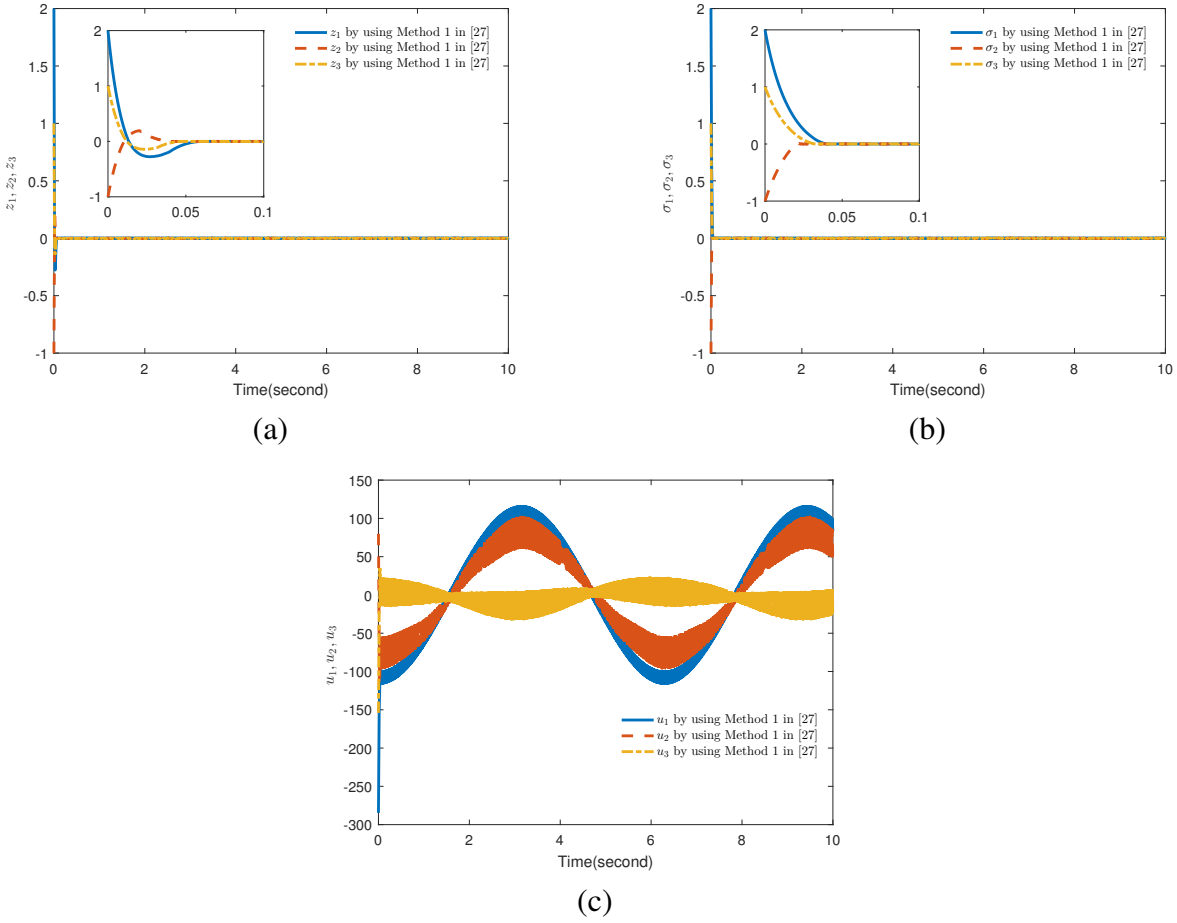

Figure 2. (a) z_1, z_2 and z_3; (b) σ_1, σ_2 and σ_3; (c) u_1, u_2 and u_3 by using Method 1 in [27].

Obviously, Figure 2 shows that *Method 1* in [27] can achieve that tracking errors z_1, z_2 and z_3 approach the origin within the predefined 0.2 seconds. However, there are two points that need improvement: 1) The nonlinear function $g_i(\boldsymbol{\zeta})$ and two upper bounds ϕ_i and C_i may be unknown rather than known. If $g_i(\boldsymbol{\zeta})$, $\Delta g_i(\boldsymbol{\zeta})$ and d_i are regarded as the mixed disturbance $\bar{d}_i(t, \boldsymbol{\zeta})$, a disturbance observer needs to be designed to estimate $\bar{d}_i(t, \boldsymbol{\zeta})$ effectively; 2) the chattering phenomenon of the controllers u_1, u_2 and u_3 needs to alleviate. To improve the above two issues, the proposed control method in this article is as follows:

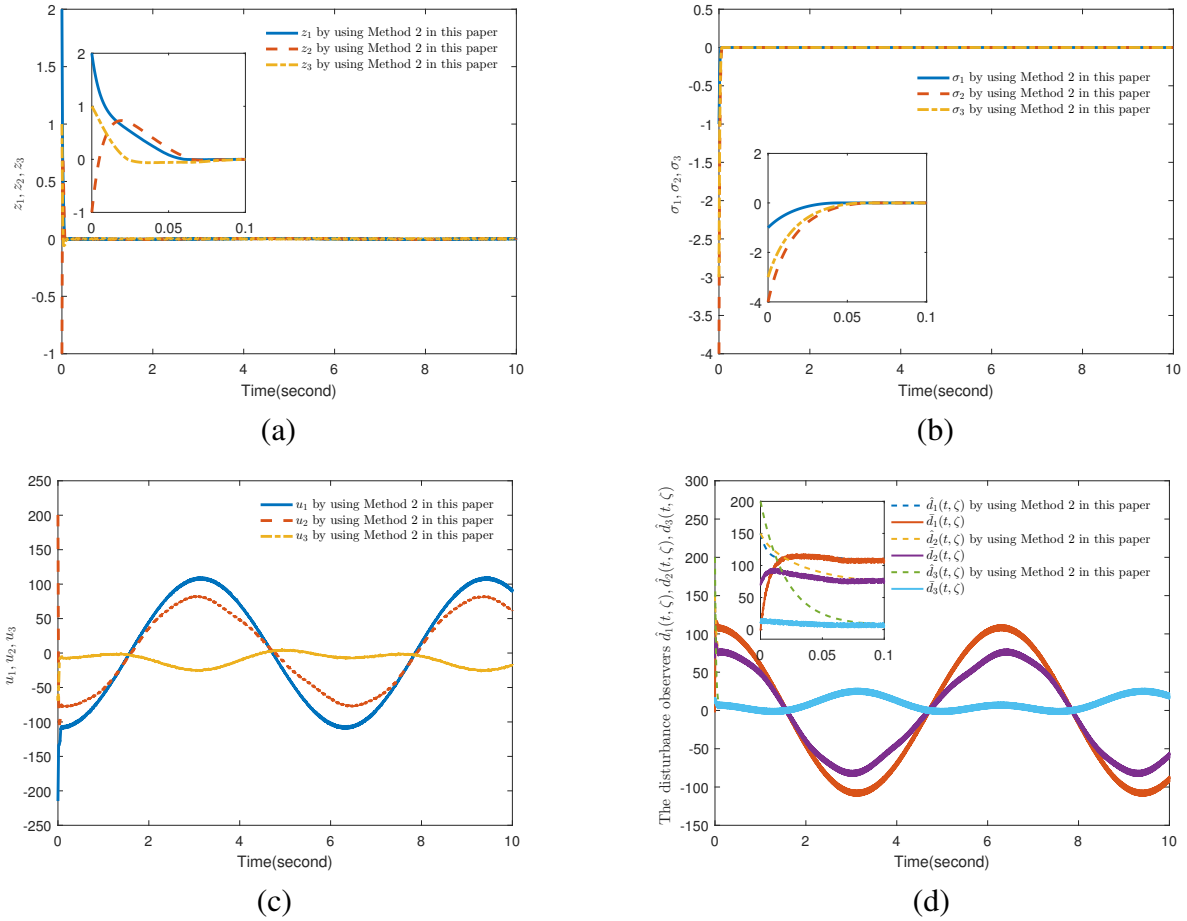

Figure 3. (a) z_1, z_2 and z_3; (b) σ_1, σ_2 and σ_3; (c) u_1, u_2 and u_3; (d) $\hat{d}_1(t,\boldsymbol{\zeta})$, $\hat{d}_2(t,\boldsymbol{\zeta})$ and $\hat{d}_3(t,\boldsymbol{\zeta})$ by using Method 2 in this paper.

Method 2: The predefined-time control method in this paper uses (3.1) as the disturbance observer, (3.5) as the sliding surface, and (3.6) as the controller. For ζ_1, ζ_2 and ζ_3, five fuzzy sets are defined over $[-5,5]$ with partitioning points as -5; -2.5; 0; 2.5; 5. Define the vectors as $\boldsymbol{\zeta} = [\zeta_1, \zeta_2, \zeta_3]^T$ and $\boldsymbol{\zeta}_k^0 = [-7.5 + k, -7.5 + k, -7.5 + k]^T$, $k = 1, 2, 3, 4, 5$. The fuzzy membership functions are given as $\varrho_A^1(\boldsymbol{\zeta}) = \exp(\frac{-\|\boldsymbol{\zeta}-\boldsymbol{\zeta}_1^0\|^2}{2})$, $\varrho_A^2(\boldsymbol{\zeta}) = \exp(\frac{-\|\boldsymbol{\zeta}-\boldsymbol{\zeta}_2^0\|^2}{2})$, $\cdots$, $\varrho_A^5(\boldsymbol{\zeta}) = \exp(\frac{-\|\boldsymbol{\zeta}-\boldsymbol{\zeta}_5^0\|^2}{2})$. We can express $\psi_{f_1}(\boldsymbol{\zeta})$, $\psi_{f_2}(\boldsymbol{\zeta})$ and $\psi_{f_3}(\boldsymbol{\zeta})$ as $\psi_{f_1}(\boldsymbol{\zeta}) = \psi_{f_2}(\boldsymbol{\zeta}) = \psi_{f_3}(\boldsymbol{\zeta}) = [\psi^1(\boldsymbol{\zeta}), \cdots, \psi^5(\boldsymbol{\zeta})]^T$, where $\psi^k(\boldsymbol{\zeta}) = \frac{\varrho_A^k(\boldsymbol{\zeta})}{\sum_{k=1}^{5} \varrho_A^k(\boldsymbol{\zeta})}$. The parameters $T_{c_1}, T_{c_2}, q_1 = 0.5, q_2 = 0.25, b_1, b_2, b_3$ and b_4 remain the same as those in *Method 1*. In addition, other parameters are selected as $\beta_1 = \beta_2 = \beta_3 = 50$, $\rho_1 = \rho_2 = \rho_3 = 2, \lambda_1 = \lambda_2 = \lambda_3 = 0.5$. Initial values are selected as $s_1(0) = s_2(0) = s_3(0) = 0$, $\hat{\theta}_{f_1}(0) = \hat{\theta}_{f_2}(0) = \hat{\theta}_{f_3}(0) = 0$. Simulation results of *Method 2* are depicted in Figure 3. As shown in Figure 3, the proposed *Method 2* can overcome the influence of unknown mixed disturbances $\bar{d}_1(t,\boldsymbol{\zeta})$, $\bar{d}_2(t,\boldsymbol{\zeta})$ and $\bar{d}_3(t,\boldsymbol{\zeta})$ and ensure that tracking errors z_1, z_2 and z_3 approach the neighborhood near the origin within 0.3 seconds, and the chattering phenomenon of controllers u_1, u_2 and u_3 is greatly reduced. Meanwhile, the designed disturbance observers $\hat{d}_1(t,\boldsymbol{\zeta})$, $\hat{d}_2(t,\boldsymbol{\zeta})$ and $\hat{d}_3(t,\boldsymbol{\zeta})$ can effectively estimate the corresponding mixed disturbances $\bar{d}_1(t,\boldsymbol{\zeta})$, $\bar{d}_2(t,\boldsymbol{\zeta})$ and

$\bar{d}_3(t,\boldsymbol{\zeta})$. Therefore, one can conclude that the presented method has better performance.

4.1. Robustness test

This part verifies the anti-interference ability and robustness of the presented approach, and analyzes it in the absence or presence of random disturbance noise and uncertainty. When the system (2.1) is not affected by the random noise disturbance and internal system uncertainty, and nonlinear functions $g_1(\boldsymbol{\zeta})$, $g_2(\boldsymbol{\zeta})$ and $g_3(\boldsymbol{\zeta})$ are known, the sliding mode manifold and controller design of *Method 2* in this paper are as follows:

$$\begin{aligned}\sigma_i &= z_i + \int_0^t (\tfrac{1}{q_1}\tfrac{\pi}{T_{c_1}}(\tfrac{1}{2})^{1-\frac{q_1}{2}}\mathrm{sgn}(z_i(\tau))|z_i(\tau)|^{1-q_1} \\ &\quad + \tfrac{1}{q_1}\tfrac{\pi}{T_{c_1}}(\tfrac{1}{2})^{1+\frac{q_1}{2}}\mathrm{sgn}(z_i(\tau))|z_i(\tau)|^{1+q_1})\mathrm{d}\tau,\end{aligned} \tag{4.4}$$

and

$$\begin{aligned}u_i &= \dot{x}_{d_i} - \tfrac{1}{q_1}\tfrac{\pi}{T_{c_1}}(\tfrac{1}{2})^{1-\frac{q_1}{2}}\mathrm{sgn}(z_i)|z_i|^{1-q_1} - \tfrac{1}{q_1}\tfrac{\pi}{T_{c_1}}(\tfrac{1}{2})^{1+\frac{q_1}{2}}\mathrm{sgn}(z_i)|z_i|^{1+q_1} \\ &\quad -g_i(\boldsymbol{\zeta}) - \tfrac{1}{q_2}\tfrac{\pi}{T_{c_2}}(\tfrac{1}{2})^{2-q_2}\mathrm{sgn}(\sigma_i)|\sigma_i|^{1-2q_2} \\ &\quad -\tfrac{1}{q_2}\tfrac{\pi}{T_{c_2}}(\tfrac{1}{2})^{2+q_2}\mathrm{sgn}(\sigma_i)|\sigma_i|^{1+2q_2},\end{aligned} \tag{4.5}$$

Select the initial value and control parameters as the same as the previous ones. The simulation result is shown in Figure 4.

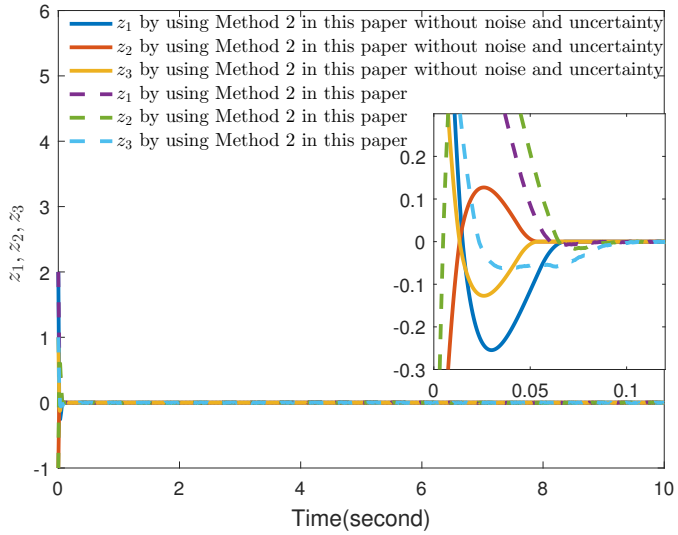

Figure 4. Robustness test of the proposed method.

Figure 4 shows that the proposed method has good anti-interference and robustness in the presence of noise and internal system uncertainty.

5. Conclusions

This article presents a predefined-time SMC strategy for tracking n-dimensional CSs under uncertainties and disturbances. First, a disturbance observer and a novel sliding manifold are derived.

Second, a sliding mode controller is developed for CSs. The predefined time is not affected by the initial conditions and can be set arbitrarily according to actual needs. The main difference from fixed-time control is that it can pre-allocate convergence time, so that the proposed method can meet the practical requirements of predefined convergence time even in the presence of internal uncertainties and random noise disturbances. The simulation results confirm the effectiveness and robustness of the method proposed in this paper.

Use of AI tools declaration

The authors declare they have not used Artificial Intelligence (AI) tools in the creation of this article.

Acknowledgments

This work was supported in part by Anhui province university excellent talents funding project (gxbjZD2021075) and in part by the Natural Science Foundation for the Higher Education Institutions of Anhui Province (2023AH051549).

Conflict of interest

The authors declare there is no conflict of interest.

References

1. M. C. Ho, Y. C. Hung, Z. Y. Liu, I. M. Jiang, Reduced-order synchronization of chaotic systems with parameters unknown, *Phys. Lett. A*, **348** (2006), 251–259. https://doi.org/10.1016/j.physleta.2005.08.076
2. L. M. Pecora, T. L. Carroll, Synchronization in chaotic systems, *Phys. Rev. Lett.*, **64** (1990), 821. https://doi.org/10.1103/PhysRevLett.64.821
3. S. Ha, L. Y. Chen, H. Liu, Command filtered adaptive neural network synchronization control of fractional-order chaotic systems subject to unknown dead zones, *J. Franklin Inst.*, **358** (2021),3376–3402. https://doi.org/10.1016/j.jfranklin.2021.02.012
4. H. Bao, Z. Y. Hua, N. Wang, L. Zhu, M. Chen, B. C. Bao, Initials-boosted coexisting chaos in a 2-d sine map and its hardware implementation, *IEEE Trans. Ind. Inf.*, **17** (2020), 1132–1140. https://doi.org/10.1109/TII.2020.2992438
5. A. Altan, S. Karasu, S. Bekiros, Digital currency forecasting with chaotic meta-heurist bio-inspired signal processing techniques, *Chaos Solitons Fractals*, **126** (2019), 325–336. https://doi.org/10.1016/j.chaos.2019.07.011
6. C. H. Lin, C. W. Ho, G. H. Hu, B. Sreeramaneni, J. J. Yan, Secure data transmission based on adaptive chattering-free sliding mode synchronization of unied chaotic systems, *Mathematics*, **21** (2021), 2658. https://doi.org/10.3390/math9212658
7. G. W. Xu, S. D. Zhao, Y. Cheng, Chaotic synchronization based on improved global nonlinear integral sliding mode control, *Comput. Electr. Eng.*, **96** (2021), 107497. https://doi.org/10.1016/j.compeleceng.2021.107497

8. A. Izadbakhsh, N. Nikdel, Chaos synchronization using differential equations as extended state observer, *Chaos Solitons Fractals*, **153** (2021), 111433. https://doi.org/10.1016/j.chaos.2021.111433

9. N. Cai, W. Q. Li, Y. W. Jing, Finite-time generalized synchronization of chaotic systems with different order, *Nonlinear Dyn.*, **64** (2011), 385–393. https://doi.org/10.1007/s11071-010-9869-1

10. X. Y. Chen, T. W. Huang, J. D. Cao, J. H. Park, J. L. Qiu, Finite-time multi-switching sliding mode synchronisation for multiple uncertain complex chaotic systems with net-work transmission mode, *IET Control Theory Appl.*, **13** (2019), 1246–1257. http://dx.doi.org/10.1049/iet-cta.2018.5661

11. W. G. Ao, T. D. Ma, R. V. Sanchez, H. T. Gan, Finite-time and fixed-time impulsive synchronization of chaotic systems, *J. Franklin Inst.*, **357** (2020), 11545–11557. https://doi.org/10.1016/j.jfranklin.2019.07.023

12. D. Zhang, J. Mei, P. Miao, Global finite-time synchronization of different dimensional chaotic systems, *Appl. Math. Modell.*, **48** (2017), 303–315. https://doi.org/10.1016/j.apm.2017.04.009

13. Q. J. Yao, Synchronization of second-order chaotic systems with uncertainties and disturbances using fixed-time adaptive sliding mode control, *Chaos Solitons Fractals*, **142** (2021), 110372. https://doi.org/10.1016/j.chaos.2020.110372

14. M. Dutta, B. K. Roy, A new memductance-based fractional-order chaotic system and its fixed-time synchronisation, *Chaos Solitons Fractals*, **145** (2021), 110782. https://doi.org/10.1016/j.chaos.2021.110782

15. Y. M. Sun, F. Wang, Z. Liu, Y. Zhang, C. P. Chen, Fixed-time fuzzy control for a class of nonlinear systems, *IEEE Trans. Cyber.*, **52** (2020), 3880–3887. https://doi.org/10.1109/TCYB.2020.3018695

16. S. Z. Xie, Q. Chen, Adaptive nonsingular predfiened-time control for attitude stabilization of rigid spacecrafts, *IEEE Trans. Circuits Syst. II Express Briefs*, **69** (2021), 189–193. https://doi.org/10.1109/TCSII.2021.3078708

17. Y. Sun, Y. Gao, Y. Zhao, Z. Liu, J. Wang, J. Kuang, et al., Neural network-based tracking control of uncertain robotic systems: Predefined-time nonsingular terminal sliding-mode approach, *IEEE Trans. Ind. Electron.*, **69** (2020), 10510–10520. https://doi.org/10.1109/TIE.2022.3161810

18. Y. Wang, H. Y. Li, Y. Guan, M. S. Chen, Predefine-time chaos synchronization of memristor chaotic systems by using simplified control inputs, *Chaos Solitons Fractals*, **161** (2022), 112282. https://doi.org/10.1016/j.chaos.2022.112282

19. E. A. Assali, Predefined-time synchronization of chaotic systems with different dimensions and applications, *Chaos Solitons Fractals*, **147** (2021), 110988. https://doi.org/10.1016/j.chaos.2021.110988

20. E. R. Wang, S. H. Yan, Q. Y. Wang, A new four-dimensional chaotic system with multistability and its predefined-time synchronization, *Int. J. Bifurcation Chaos*, **32** (2022), 2250207. https://doi.org/10.1142/S0218127422502078

21. H. B. Xue, X. H. Liu, A novel fast terminal sliding mode with predefined-time synchronization, *Chaos Solitons Fractals*, **175** (2023), 114049. https://doi.org/10.1016/j.chaos.2023.114049

22. C. A. Anguiano-Gijón, A. J. Muñoz-Vázquez, J. D. Sánchez-Torres, G. Romero-Galván, F. Martínez-Reyes, On predefined-time synchronisation of chaotic systems, *Chaos Solitons Fractals*, **122** (2019), 172–178. https://doi.org/10.1016/j.chaos.2019.03.015

23. A. J. Muñoz-Vázquez, J. D. Sánchez-Torres, C. A. Anguiano-Gijón, Single-channel predefined-time synchronisation of chaotic systems, *Asian J. Control*, **23** (2021), 190–198. https://doi.org/10.1002/asjc.2234

24. M. J. Zhang, H. Y. Zang, L. Y. Bai, A new predefined-time sliding mode control scheme for synchronizing chaotic systems, *Chaos Solitons Fractals*, **14** (2022), 112745. https://doi.org/10.1016/j.chaos.2022.112745

25. J. K. Ni, C. X. Liu, K. Liu, L. Liu, Finite-time sliding mode synchronization of chaotic systems, *Chin. Phys. B*, **23** (2014), 100504. https://doi.org/10.1088/1674-1056/23/10/100504

26. M. Shirkavand, M. Pourgholi, Robust fixed-time synchronization of fractional order chaotic using free chattering nonsingular adaptive fractional sliding mode controller design, *Chaos Solitons Fractals*, **113** (2018), 135–147. https://doi.org/10.1016/j.chaos.2018.05.020

27. Q. P. Li, C. Yue, Predefined-time polynomial-function-based synchronization of chaotic systems via a novel sliding mode control, *IEEE Access*, **8** (2020), 162149–162162. https://doi.org/10.1109/ACCESS.2020.3021094

28. P. Li, L. Di, B. Simone, Boundary-layer control with unstructured uncertainties with application to adaptive autopilots, *IEEE Trans. Control Syst. Technol.*, **2023** (2023). https://doi.org/10.1109/TCST.2023.3329908

29. J. Zhao, Y. F. Lv, Output-feedback robust tracking control of uncertain systems via adaptive learning, *Int. J. Control Autom. Syst.*, **21** (2023), 1108–1118. https://doi.org/10.1007/s12555-021-0882-6

30. Y. X. Wang, Heterogeneous network representation learning approach for ethereum identity identification, *IEEE Trans. Comput. Soc. Syst.*, **10** (2022), 890–899. https://doi.org/10.1109/TCSS.2022.3164719

31. W. Qi, S. E. Ovur, Z. Li, A. Marzullo, R. Song, Multi-sensor guided hand gesture recognition for a teleoperated robot using a recurrent neural network, *IEEE Rob. Autom. Lett.*, **6** (2021), 6039–6045. https://doi.org/10.1109/LRA.2021.3089999

32. M. P. Aghababa, S. Khanmohammadi, G. Alizadeh, Finite-time synchronization of two different chaotic systems with unknown parameters via sliding mode technique, *Appl. Math. Modell.*, **35** (2011), 3080–3091. https://doi.org/10.1016/j.apm.2010.12.020

33. X. Z. Guo, G. G. Wen, Z. X. Peng, Y. L. Zhang, Global fixed-time synchronization of chaotic systems with different dimensions, *J. Franklin Inst.*, **357** (2020), 1155–1173. https://doi.org/10.1016/j.jfranklin.2019.11.063

34. J. D. Sánchez-Torres, D. Gómez-Gutiérrez, E. López, A. G. Loukianov, A class of predefined-time stable dynamical systems, *IMA J. Math. Control Inf.*, **35** (2018), 1–29. https://doi.org/10.1093/imamci/dnx004

35. A. J. Munoz-Vazquez, J. D. Sanchez-Torres, M. l. Defoort, S, Boulaaras, Predefined-time convergence in fractional-order systems, *Chaos Solitons Fractals*, **143** (2021), 110571. https://doi.org/10.1016/j.chaos.2020.110571

36. Q. Wang, J. D. Cao, H. Liu, Adaptive fuzzy control of nonlinear systems with predefined time and accuracy, *IEEE Trans. Fuzzy Syst.*, **30** (2022), 5152–5165. https://doi.org/10.1109/TFUZZ.2022.3169852

37. S. Sahoo, B. K. Roy, Design of multi-wing chaotic systems with higher largest lyapunov exponent, *Chaos Solitons Fractals*, **157** (2022),111926. https://doi.org/10.1016/j.chaos.2022.111926

AIMS Press